Heliyon 9 (2023) e22281

Contents lists available at ScienceDirect

Heliyon

journal homepage: www.cell.com/heliyon

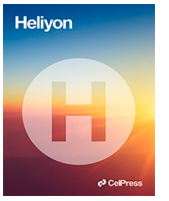

RNA binding proteins PTBP1 and HNRNPL regulate *CFTR* mRNA decay

Amna Siddiqui [a,b,c], Arpit Saxena [a,b], Joshua Echols [a,b,d], Viktoria Havasi [a,b,c], Lianwu Fu [a,b], Kim M. Keeling [a,b,*]

[a] *Department of Biochemistry and Molecular Genetics and, USA*
[b] *Gregory Fleming James Cystic Fibrosis Research Center, University of Alabama at Birmingham Heersink School of Medicine, Birmingham, AL 35294, USA*
[c] *Comprehensive Cancer Center and, USA*
[d] *Department of Pediatrics, Infectious Diseases Division, University of Alabama at Birmingham Heersink School of Medicine, Birmingham, AL 35294, USA*

ARTICLE INFO

Keywords:
CFTR
PTBP1
HNRNPL
Nonsense-mediated mRNA decay
mRNA abundance

ABSTRACT

Background: CFTR nonsense alleles generate negligible CFTR protein due to the nonsense mutation: 1) triggering *CFTR* mRNA degradation by nonsense-mediated mRNA decay (NMD), and 2) terminating *CFTR* mRNA translation prematurely. Thus, people with cystic fibrosis (PwCF) who carry nonsense alleles cannot benefit from current modulator drugs, which target CFTR protein. In this study, we examined whether PTBP1 and HNRNPL, two RNA binding proteins that protect a subset of mRNAs with a long 3' untranslated region (UTR) from NMD, similarly affect *CFTR* mRNA.

Silencing RNAs were used to deplete PTBP1 or HNRNPL in 16HBE14o- human bronchial epithelial cells expressing WT, G542X, or W1282X *CFTR*. *CFTR* mRNA abundance was measured relative to controls by quantitative PCR. PTBP1 and HNRNPL were also exogenously expressed in each cell line and *CFTR* mRNA levels were similarly quantified.

Results: PTBP1 depletion reduced *CFTR* mRNA abundance in all three 16HBE14o- cell lines; HRNPL depletion reduced *CFTR* mRNA abundance in only the G542X and W1282X cell lines. Notably, decreased *CFTR* mRNA abundance correlated with increased mRNA decay. Exogenous expression of PTBP1 or HNRNPL increased *CFTR* mRNA abundance in all three cell lines; HNRNPL overexpression generally increased *CFTR* to a greater extent in G542X and W1282X 16HBE14o- cells.

Our data indicate that PTBP1 and HNRNPL regulate *CFTR* mRNA abundance by protecting *CFTR* transcripts from NMD. This suggests that PTBP1 and/or HNRNPL may represent potential therapeutic targets to increase *CFTR* mRNA abundance and enhance responses to CFTR modulators and other therapeutic approaches in PwCF.

1. Introduction

Modulator drugs target defective cystic fibrosis transmembrane conductance regulator (CFTR) protein to rescue its proper

* Corresponding author. Address: Room 444 BBRB, 845 19th Street South, Birmingham, AL 35205, USA.
E-mail address: kkeeling@uab.edu (K.M. Keeling).

https://doi.org/10.1016/j.heliyon.2023.e22281
Received 25 September 2023; Received in revised form 7 November 2023; Accepted 8 November 2023
Available online 13 November 2023

localization and function, providing potential therapeutic benefits in ~90 % of people with cystic fibrosis (PwCF) [1]. Most of the remaining ~10 % of PwCF carry a nonsense mutation that abrogates CFTR expression, and thus, are unresponsive to modulators. A nonsense mutation generates an in-frame premature termination codon (PTC) in the *CFTR* mRNA, leading to negligible CFTR protein expression/function by: 1) triggering nonsense-mediated mRNA decay (NMD), and 2) ending translation before a full-length, functional protein is produced.

CFTR mRNA expression from PTC-containing alleles is generally reduced to 5–30 % of normal due to NMD [2], a cellular pathway that degrades mRNAs harboring a PTC. By significantly reducing *CFTR* mRNA abundance, NMD limits the effectiveness of therapeutic strategies aimed at rescuing CFTR protein expression/function from PTC-containing alleles, including nonsense suppression therapies using small molecules or suppressor tRNAs, or mRNA-targeted allele specific oligonucleotide (ASO) or mutation repair methodologies [3,4]. Inhibiting NMD to maintain *CFTR* mRNA abundance is potentially one way to enhance therapies that target PTCs. However, little is known about how *CFTR* mRNAs are targeted for NMD.

It was recently shown by the Hogg group that mRNA binding proteins polypyrimidine tract binding protein 1 (PTBP1) [5,6] and heterogeneous nuclear ribonucleoprotein L (HNRNPL) [7] can displace the UPF1 NMD factor from the 3' UTR of certain mRNAs, protecting those transcripts from NMD. In this study, we examined whether PTBP1 and HNRNPL similarly regulate *CFTR* mRNA.

PTBP1 and HNRNPL knockdowns led to significant decreases in *CFTR* mRNA abundance in G542X and W1282X 16HBE14o- (16HBE) cells. PTBP1 depletion also decreased *CFTR* mRNA in wild-type (WT) 16HBEs, but HNRNPL depletion had no effect. mRNA half-life studies showed decreases in *CFTR* mRNA abundance correlated with increased rates of mRNA turnover. Exogenous expression of PTBP1 and HNRNPL led to significant increases in *CFTR* mRNA abundance in all three cell lines, with HNRNPL expression yielding a more pronounced effect in G542X and W1282X 16HBEs than in WT cells. Together, our data suggest that PTBP1 and HNRNPL regulate *CFTR* mRNA abundance by protecting *CFTR* transcripts from NMD, but likely *via* different mechanisms.

2. Materials and methods

Cell culture: Immortalized, human bronchial epithelia cell lines 16HBE14o- (16HBE) expressing WT, G542X, or W1282X *CFTR* were generated by the Cystic Fibrosis Foundation Therapeutics (CFFT) Lab [8] and distributed to the UAB CF Research Center. The cells were authenticated and tested for mycoplasma prior to use (IDEXX BioAnalytics). 16HBEs were maintained in culture at 37 °C with 6.5 % CO_2 in minimum essential medium containing Earle's balanced salt solution non-essential amino acids, 2 mM L-glutamine, 1 mM sodium pyruvate, 1500 mg/L sodium bicarbonate (ATCC 30–2003), 100 units/mL penicillin/streptomycin (Corning Cellgro 30-002-Cl), and 10 % (v/v) fetal bovine serum (Atlanta Biologicals S11150). Cells were seeded into plates precoated with FNC (Athena Enzyme System 0407). PET Cold Trypsin Cell Release Reagent (Athena Enzyme System 0405) was used to detach cells.

Generation of 16HBEs stably expressing the PTBP1 or HNRNPL isoforms: Isoforms of PTBP1 and HNRNPL carrying a C-terminal hemagglutinin (HA) epitope tag from the pcDNA3.1(+) vector were purchased from GenScript Biotech Corporation. DNA fragments containing HA-tagged PTBP1 or HNRNPL were isolated after *Bam*HI/*Nsi*I digestion and cloned into the *Bam*HI/*Nsi*I sites of the pLenti-puro vector (Addgene 39481) [9]. The resulting transfer vectors were packaged into lentiviral particles after transfecting pMD2.G (pMD2.G was a gift from Didier Trono, Addgene 12259), pMDLg/pRRE (Addgene 12251) and pRSV-REV (Addgene 12253) *(10)* into HEK293T cells using Lipofectamine 3000 transfection reagent (Invitrogen L3000008). The lentiviral particles were then transduced into 16HBEs [10]. 48 h post-transduction, selection medium (growth medium containing 1 μg/ml puromycin) was used to select for stably transduced cells.

Transfection of siRNAs: Silencing RNAs (siRNAs) were transfected into 16HBEs using Lipofectamine RNAiMAX Reagent (Thermo Fisher Scientific 13-778-150) according to manufacturer instructions. Between 60 and 90 pmol of each siRNA was used to obtain efficient knockdowns while minimizing cell death (Supplementary Fig. 7). siRNAs were obtained from Thermo Fisher Scientific: scrambled control (4390844); PTBP1 (s11435); HNRNPL (s6741); UPF1 (s11927); UPF2 (s24948); UPF3B (s535067). 72 h after transfection, cells were harvested for assay.

Cell viability: Cell viability was monitored using the Cell Titer Glo Luminescent Cell Viability Assay (Promega G2943). 16HBE cells were seeded per well into a FNC (Athena Enzyme System 0407) coated, black, clear-bottom 96-well culture plate (Corning 3603) and assayed after treatment according to manufacturer instructions using a GloMax Multi-Detection System (Promega).

Reverse Transcription (RT) and Quantitative PCR (qPCR): Total RNA was extracted from 16HBEs using a Ribopure RNA Purification Kit (Ambion PR-M9004) and then DNase-treated using the Turbo DNA-Free Kit (Thermo Fisher Scientific AM1907). Polyadenylated RNA was reverse transcribed into cDNA in a 50 μL reaction containing 2 μg of total RNA; 0.5 μg/μL oligo dT; 10 mM dNTPs; 40U/μL RNasin (Promega N2511); 10 μL of 5X AMV RT buffer and 40 U/μL AMV reverse transcriptase (Promega PR-M9004). Reverse transcription (RT) reactions were incubated at 42 °C for 1.5 h and then heat inactivated at 65 °C for 15 min cDNA was subjected to qPCR in a 25 μL reaction containing 12.5 μL iQ SYBR Green Supermix (Bio-Rad 1708882); 10 μM of each forward and reverse primer; and 2 μg of cDNA. qPCR was performed with a Bio-Rad CFX96 Real-Time PCR Detection System using a program that included an initial 3-min denaturation step at 95 °C followed by 40 repeated cycles of a 10 s denaturation step at 95 °C and a 30 s annealing/extension step at 60 °C. Melt curve analysis was initially performed with each primer set to verify that only one gene product was generated from the PCR reactions; a standard curve was performed using each primer set to ensure PCR efficiency ranged between 90 and 110 %. Average quantification cycle (Cq) values were used for quantification using the Livak (ΔΔCq) method [11], where *KRT18* or *PPIA* were used as normalization controls. qPCR primer sequences used include: ALX: Forward = 5′-CAGCGAAGCCTGCATGT-3′, Reverse = 5′-TTGGCGTTATGGGCTTCG-3'; BCL2: Forward = 5′-GGAGGATTGTGGCCTTCTTT-3′, Reverse = 5′ GTTCAGGTACTCAGTCATCCACAGG-3'; CFTR: Forward = 5′-GAGGGTA

AAATTAAGCACAGT-3′, Reverse = 5′-TGCTCGTTGACCTCCA-3'; HNRNPL: Forward =

5′-CAATCTAAGATGAACTGTGACC-3′, Reverse = 5′-TCATGAATTTCACCTTCTCC-3’;
KRT18: Forward = 5′-AGTCTGTGGAGAACGACATCC-3′, Reverse = 5′-TGGTGCTCTCC
TCAATCTGC-3’; PPIA: Forward = 5′-GGCAAATGCTGGACCCAACACA-3′, Reverse = 5′-TGCTGGTCTTGCCATTCCTGGA-3’; PTBP1: Forward = 5′-GTTGGGAGAGCTGTCGGT
CTT-3′, Reverse = 5′-ACCAGGCCTTCATCGAGAT-3’; UPF1: Forward = 5′-ACCTATTAC
ACGAAGGACCT C-3′, Reverse = 5′-ACGTCCGTTGCAGAACCAC-3’; UPF2: Forward =

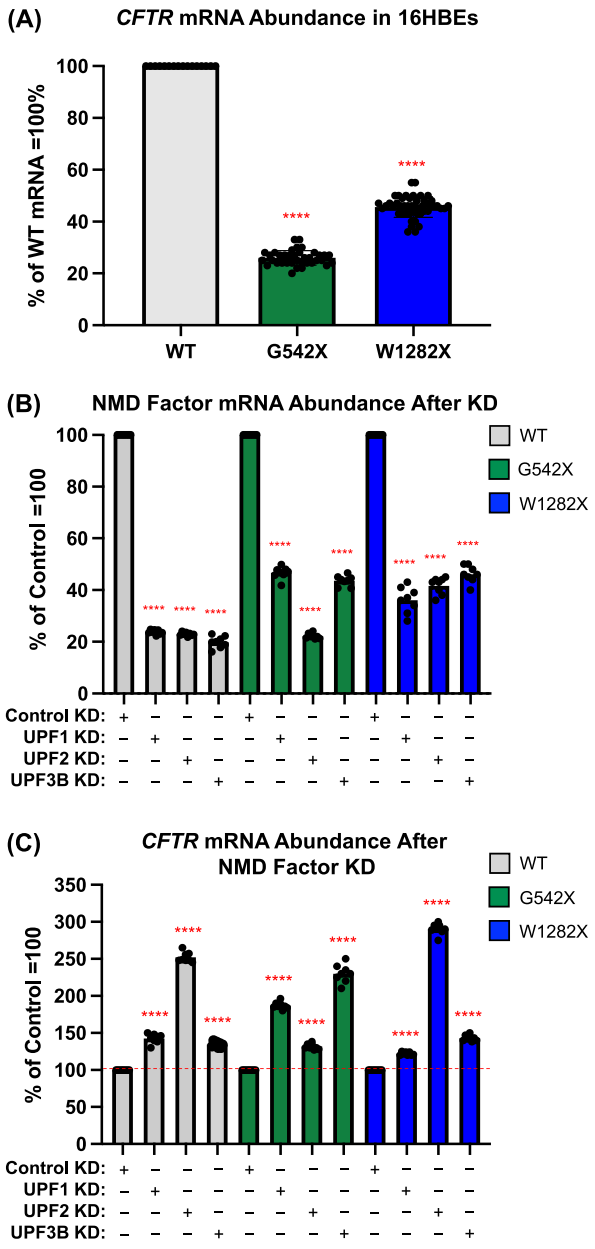

Fig. 1. Characterizing NMD of *CFTR* mRNAs carrying different PTCs in 16HBE14o- (16HBE) cells. **(A)** qPCR data quantifying human *CFTR* mRNA abundance in G542X and W1282X 16HBEs relative to wild-type (WT) 16HBEs (=100 %). **(B)** qPCR data quantifying the mRNA abundance of the human NMD factors UPF1, UPF2, and UPF3B after their knockdown (KD) in WT, G542X, or W1282X 16HBEs. The mRNA abundance for each depleted factor is expressed relative to the scrambled control for each cell line (=100 %). **(C)** qPCR data quantifying *CFTR* mRNA abundance in each 16HBE cell line after NMD factor knockdown relative to the scrambled siRNA control (=100 %). For panels A–C, each column represents the mean ± SD of the change in mRNA. For panel A, 4–6 experiments were performed in quadruplicate and normalized to *KRT18* and *PPIA*; each symbol indicates a single data point (n = 36–48); for panels B & C, two independent experiments were performed in quadruplicate and normalized to *KRT18* and *PPIA* (n = 16). Statistical analysis was performed using the Welch's unpaired *t*-test; **** indicates $p < 0.0001$ when comparing an experimental cohort with its associated control (WT control in panel A, and the scrambled control for each cell line in panels B and C).

5′-GTCCTGGGTCACATAATG-3′, Reverse = 5′-CTCCTTGCTGCTCACTG-3’; UPF3B:
Forward = 5′-CAGGATCGCAACAAGGAGAAG-3′, Reverse = 5′-TCAGGCATAGGTTGA AGATGTTC-3’.

Western blotting: Cell lysates were generated using M-Per Mammalian Protein Extraction Reagent (Thermo Fisher Scientific P178501). 25 μg of total protein per sample was subjected to SDS-PAGE and transferred to 0.45 μm Immobilon FL Transfer Membrane (Thermo Fisher Scientific IPFL00010). After blocking, blots were incubated with the following antibodies according to manufacturer instructions: UPF1 (Abcam 109363), UPF2 (Thermo-Fisher Scientific PIPA577128), UPF3 (Thermo-Fisher Scientific PA541903), PTBP1 (Thermo Fisher Scientific 12582-1-AP), HNRNPL (Abcam ab6106), HSP90 (Thermo Fischer Scientific 13171-1-AP), Hemagglutinin (HA) 11 epitope (Covance Research Products 901515). Bands were visualized using fluorescently labelled LI-COR Goat anti-Mouse IgG (LI-COR Biosciences 925–32210) or Goat anti-Rabbit IgG (H + L) (LI-COR Biosciences 925–32211) secondary antibodies. Protein bands were detected and quantitated using the LI-COR Biosciences Odyssey CLX Imaging System.

mRNA decay assay: 16HBEs were seeded into 6-well dishes, grown to around 30–40 % confluency, and transfected with a control or knockdown siRNA as described above. 48 h after transfection, 10 μg/mL of actinomycin D was added to the cultures. Total RNA was harvested at times = 0, 1, 2, 4, 8, and 24 h after actinomycin D addition, purified, reverse transcribed into cDNA, and subjected to qPCR as described above, where equal cDNA amounts were used. *KRT18* served as a control RNA. RNA levels were plotted where the amount of RNA at t = 0 was set to 100 % and the RNA remaining for each subsequent time point was expressed as the % of the time = 0 control. Linear regression analyses were performed with semi-log plots to calculate the rate of decay.

Statistics: All statistical analyses were performed using GraphPad Prism.

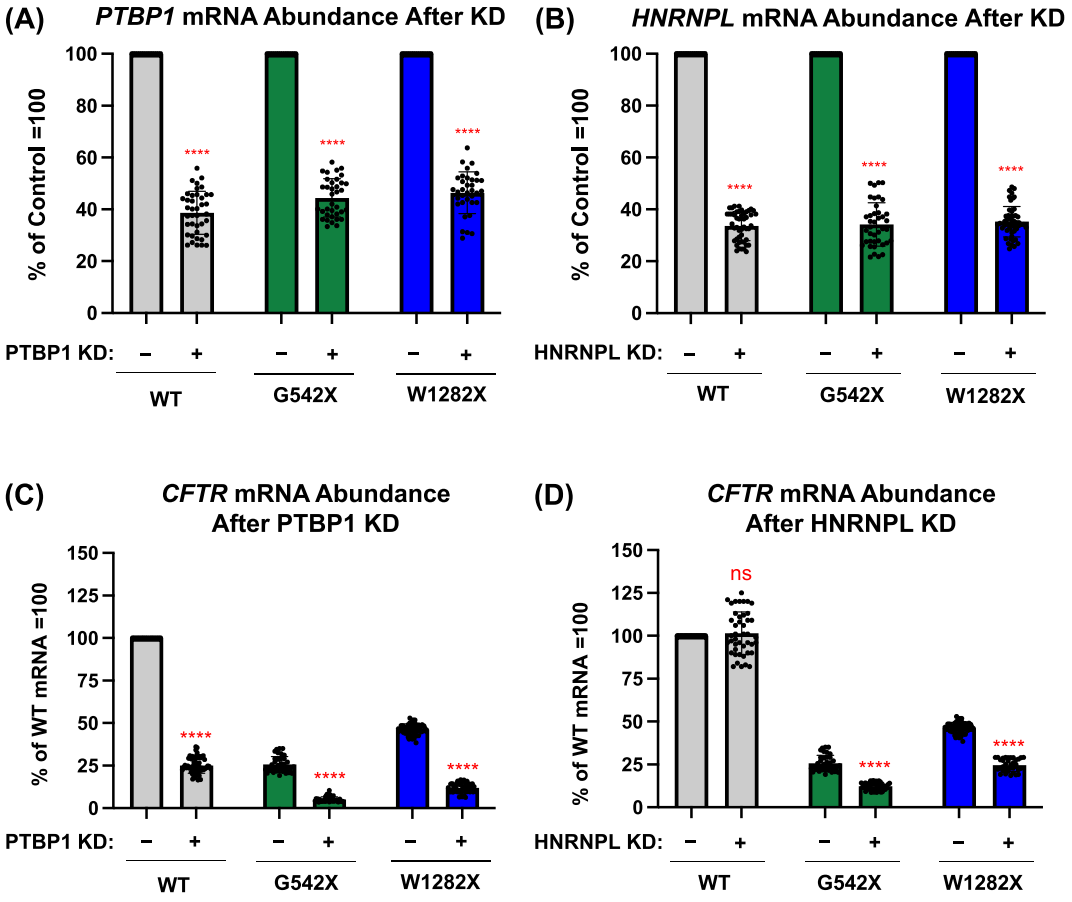

Fig. 2. *CFTR* mRNA abundance in 16HBEs after knockdown (KD) of PTBP1 or HNRNPL. (A) qPCR data quantifying *PTBP1* mRNA abundance in WT, G542X, or W1282X 16HBEs after transfection with a scrambled control siRNA (−) or a PTBP1 KD siRNA (+). **(B)** qPCR data quantifying *HNRNPL* mRNA abundance in WT, G542X, or W1282X 16HBEs after transfection with a scrambled control siRNA (−) or an HNRNPL KD siRNA (+). **(C)** qPCR data quantifying *CFTR* mRNA abundance in WT, G542X, or W1282X 16HBEs after transfection with a scrambled control siRNA (−) or a PTBP1 KD siRNA (+). **(D)** qPCR data quantifying *CFTR* mRNA abundance in WT, G542X, or W1282X 16HBEs after transfection with a scrambled control siRNA (−) or a HNRNPL KD siRNA (+). For panels A–D, each column represents the mean ± SD of changes in expression; each symbol represents an individual data point normalized to *KRT18* or *PPIA* from at least three independent experiments (n = 36–54). Data in panels A & B are expressed relative to the scrambled control for each cell line = 100 %. Data in panels C & D are expressed relative to the scrambled control for the WT cell line = 100 %. Statistical analysis was performed for panels A & B using the Welch's unpaired *t*-test. In panels C & D, statistical analysis was performed using one-way ANOVA. **** indicates $p < 0.0001$ when comparing the control with an experimental cohort.

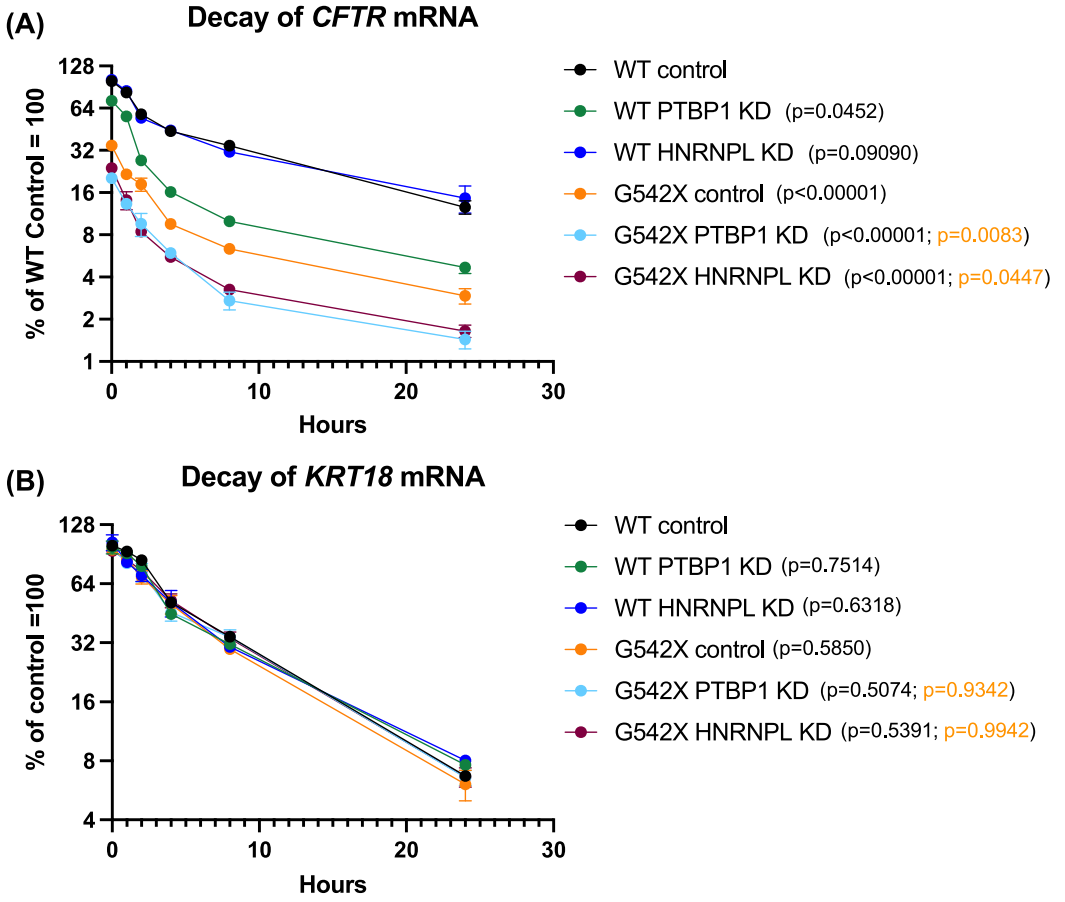

(C) Linear regression data determined from mRNA decay curves.

	CFTR		*KRT18*	
	Slope	Half-life (hr)	Slope	Half-life (hr)
WT	-2.956	4.2	-3.587	5.1
WT PTBP1 KD	-2.070	1.8	-3.530	4.8
WT HNRNPL KD	-2.955	4.1	-3.471	5.3
G542X	-0.9592	0.25	-3.384	5.1
G542X PTBP1 KD	-0.5739	0.11	-3.382	4.7
G542X HNRNPL KD	-0.6185	0.13	-3.375	5

Fig. 3. *CFTR* mRNA decay rates in 16HBEs after knockdown (KD) of PTBP1 or HNRNPL. 16HBEs expressing WT or G542X *CFTR* were transfected with 90 pmol of a scrambled, control siRNA or siRNAs to knockdown PTBP1 or HNRNPL. 48 h after siRNA transfection, 10 μg/mL of actinomycin D was added to the media and RNA was harvested at the indicated times and subjected to RT-qPCR using equal cDNA amounts to quantify the amount of: **(A)** *CFTR* or **(B)** *KRT18* remaining after actinomycin D addition relative to the control at time = 0. The data shown are the mean ± SD of the percent of mRNA remaining at each time point, where each experiment was performed twice in quadruplicate (n = 8). **(C)** Linear regression was performed using semi-log graphs to determine the rate (slope) and half-life of each decay curve, which were tested to determine whether they differed among the cohorts. In the legend, the p values in black font indicate values compared to the WT control; the p values in orange font indicate values compared to the G542X control. p values < 0.05 indicate significant differences between slopes. (For interpretation of the references to colour in this figure legend, the reader is referred to the Web version of this article.)

3. Results

3.1. Validating NMD of CFTR mRNA in 16HBEs

A previous study by Hogg & Goff [12] showed that in addition to binding at PTCs, the NMD factor UPF1 also becomes enriched on long 3′ UTRs to trigger NMD. The Hogg group recently showed a subset of transcripts with long 3′ untranslated regions (UTRs) are protected from NMD by the RNA binding proteins PTBP1 [5,6] and HNRNPL [7], which displace UPF1 from these mRNAs. We observed that the human *CFTR* mRNA has features similar to transcripts protected from NMD by PTBP1 and HNRNPL, including: 1) a 1.6 kb 3′ UTR, considered to be long relative to the median 0.6 kb 3′ UTR length among human transcripts [13], and 2) multiple CU- and CA-sites in its 3' UTR that normally reside in PTBP1 or HNRNPL RNA recognition motifs, respectively *(15)* (Supplementary Fig. 1). Based on these features, we hypothesized that PTBP1 and/or HNRNPL may regulate NMD of *CFTR* mRNAs.

We chose to use 16HBE14o- (16HBE) cells to monitor the effect of PTBP1 and HNRNPL on *CFTR* mRNA abundance. 16HBE cells are immortalized human bronchial epithelial cells that express wild-type (WT) *CFTR,* or were modified by CRISPR-Cas9 gene-editing to harbor a G542X or W1282X nonsense mutation in a *CFTR* allele [8]. Consistent with previous characterization of the 16HBE cell lines [10,14], qPCR showed steady-state *CFTR* mRNA abundance was reduced to 27 % and 46 % in G542X and W1282X 16HBEs, respectively, relative to the *CFTR* level in WT 16HBEs (Fig. 1A).

We next confirmed that the decrease of *CFTR* mRNA in the G542X and W1282X 16HBEs was a consequence of NMD. We transfected WT, G542X, and W1282X 16HBEs with either a scrambled control silencing RNA (siRNA) or siRNAs to knockdown (KD) the core NMD factors UPF1, UPF2, or UPF3B. After verifying KD efficiency at the mRNA level using qPCR (Fig. 1B) and the protein level using western blotting (Supplementary Fig. 2), we quantified *CFTR* mRNA abundance by qPCR in NMD factor depleted 16HBEs. We found that in all three 16HBE cell lines, depletion of UPF1, UPF2, or UPF3B led to significant 1.3- to 2.9-fold increases in *CFTR* mRNA abundance compared to the same cell line transfected with a scrambled control siRNA (Fig. 1C). This confirms work from previous reports that showed the G542X and W1282X nonsense mutations trigger NMD of the *CFTR* mRNA [14]. Notably, WT *CFTR* mRNA was also increased by each NMD factor KD, which was also observed in previous studies when certain NMD factors were depleted in WT 16HBEs [14,15]. This suggests that WT *CFTR* mRNA may also be subject to NMD, possibly through an EJC-independent branch of NMD that utilizes long 3' UTRs to trigger mRNA turnover.

Also consistent with previous studies [14], we observed that KD of different NMD factors had varying effects on *CFTR* mRNA abundance (Fig. 1C). For example, UPF2 KD yielded a greater increase in WT and W1282X *CFTR* mRNA abundance than KD of UPF1 or UPF3B. In contrast, KD of UPF1 and UPF3B generated a greater increase of G542X *CFTR* mRNA than UPF2 KD. These changes in *CFTR* mRNA abundance did not consistently correlate to NMD factor knockdown efficiency among the three cell lines (Fig. 1B), suggesting that the identity of the depleted NMD factor had a greater impact on rescue of *CFTR* mRNA than the modest variations in expression among NMD factors. These results are consistent with *CFTR* mRNAs being targeted to different branches of NMD based on the position of the PTC.

3.2. Knockdown (KD) of PTBP1 and HRNPL1 reduces CFTR mRNA abundance

After validating NMD of *CFTR* mRNAs in our 16HBE cell lines, we next examined the effect of depleting PTBP1 and HNRNPL on *CFTR* mRNA abundance in WT, G542X, and W1282X 16HBEs. 16HBEs were transfected with either a scrambled control siRNA or siRNAs to knockdown PTBP1 or HNRNPL. Knockdown (KD) of PTBP1 and HNRNPL1 was verified by qPCR (Fig. 2A and B) and by western blotting (Supplementary figs. 3 and 4). *CFTR* mRNA abundance in WT, G542X, and W1282X 16HBEs transfected with KD siRNAs was compared to cells transfected with the control siRNA. KD of PTBP1 resulted in a significant 4- to 6-fold decrease in *CFTR* mRNA abundance in all three 16HBE cell lines (Fig. 2C). Knockdown of HNRNPL resulted in a significant 1.9- to 2.2-fold decrease in *CFTR* mRNA abundance in G542X and W1282X 16HBEs but did not mediate a significant change in *CFTR* mRNA in WT 16HBEs (Fig. 2D). These results suggest that both PTBP1 and HNRNPL regulate the abundance of PTC-containing *CFTR* transcripts; PTBP1 also regulates WT *CFTR* mRNA abundance. Notably, the level by which PTBP1 and HNRNPL were depleted in 16HBEs *via* knock-down was sufficient to also increase the expression of *AXL* [16] and *BCL2* [17] mRNAs, whose abundance are normally down-regulated by PTBP1 and HNRNPL, respectively (Supplementary Fig. 5). PTBP1 has been shown to bind to the 5′ UTR of the *AXL* mRNA to reduce its stability (*18*), while HNRNPL destabilizes *BCL2* by binding to CA repeats in its 3' UTR (*19*). Unlike *AXL* and *BCL2*, PTBP1 and HNRNPL increase *CFTR* mRNA abundance, suggesting *CFTR* is regulated through different mechanisms than *AXL* or *BCL2*.

To determine whether PTBP1 and HNRNPL alter *CFTR* mRNA abundance by altering its stability, we examined the rate of *CFTR* mRNA decay in WT and G542X 16HBEs in which PTBP1 or HNRNPL were knocked down compared to control cells (Fig. 3A). Linear regression of semi-log decay curves was performed to determine the rate of decay and half-life of *CFTR* mRNA (Fig. 3C). We found that the rate of *CFTR* mRNA decay was significantly increased in WT and G542X 16HBEs when PTBP1 was depleted. HNRNPL depletion led to a significant increase in *CFTR* mRNA decay in the G542X cell line, but not WT. Increases in mRNA decay corresponded to decreases in mRNA half-life (Fig. 3C). Neither PTBP1 nor HNRNPL depletion significantly altered the decay rate or half-life of the control mRNA, *KRT18* (Fig. 3B) in WT or G542X 16HBEs. These results suggest that the changes in *CFTR* mRNA abundance mediated by PTBP1 and HNRNPL stem from changes in mRNA turnover, which is consistent with these proteins protecting *CFTR* mRNA from NMD.

3.3. Exogenous expression of PTBP1 and HNRPL1 increases CFTR mRNA abundance

We next examined whether exogenous expression of PTBP1 and HNRNPL affected *CFTR* mRNA abundance. Alternative splicing

events produce several isoforms of PTBP1 and HNRNPL. These variant proteins have been shown to have different mRNA binding specificity and possess non-redundant functions [18–20]. We therefore stably expressed each of the three main isoforms of PTBP1 and the two main isoforms of HNRNPL in the WT, G542X, and W1282X 16HBE cell lines. Each PTBP1 or HNRNP isoform carried a C-terminal HA epitope-tag and was expressed under strong *CMV* promoter control. Expression of each variant was verified by western blotting using an antibody to the HA epitope tag (Fig. 4A; Supplementary Fig. 6).

We next quantified *CFTR* mRNA abundance in the WT, G542X, and W1282X 16HBE cell lines expressing each mRNA binding

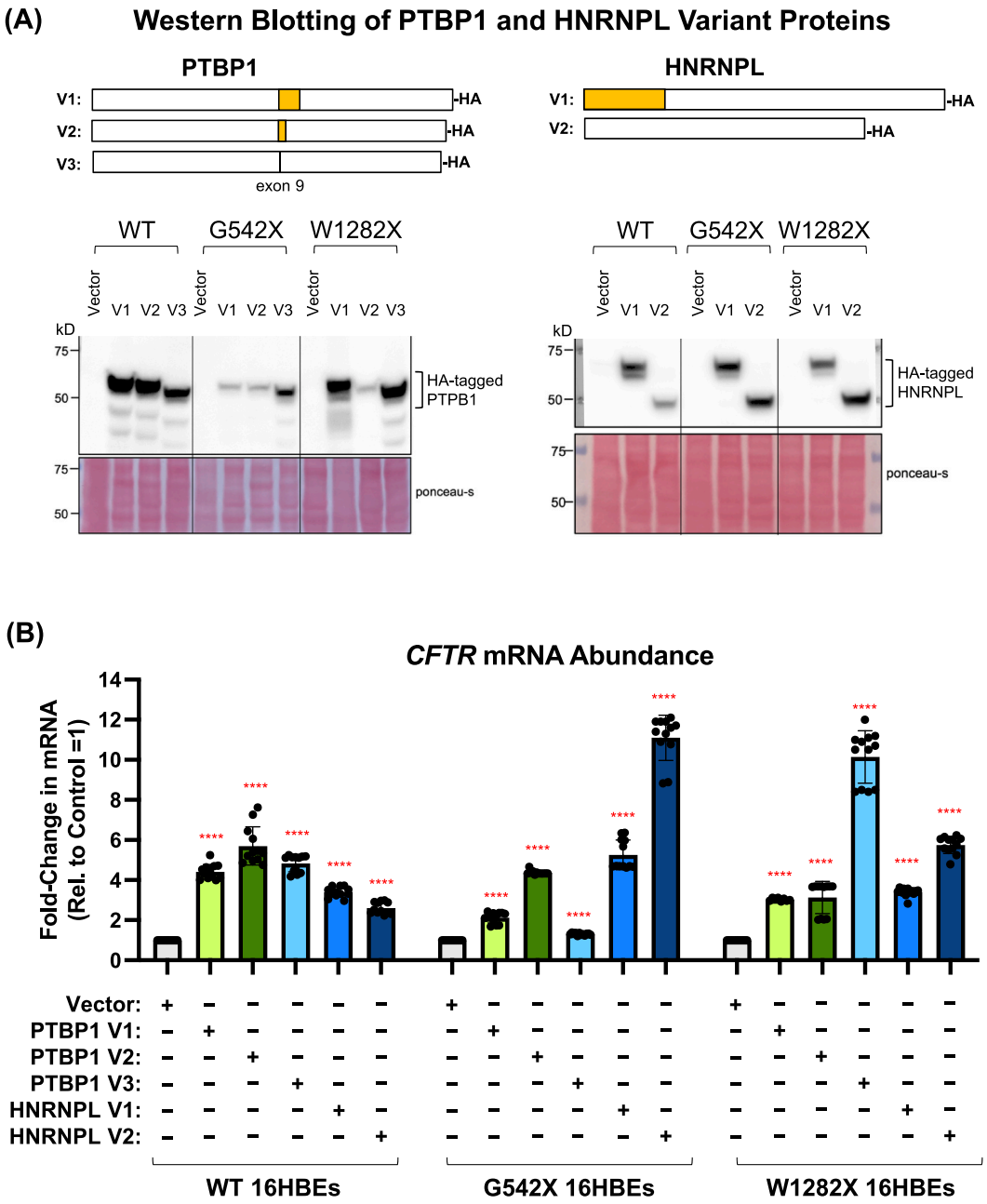

Fig. 4. ***CFTR*** **mRNA abundance in 16HBEs exogenously expressing PTBP1 and HNRNPL isoforms. (A)** Western blots of PTBP1 and HNRNPL isoforms in WT, G542X, or W1282X 16HBEs using an antibody to the C-terminal HA epitope tag. Full, non-adjusted blots are shown in Supplementary Fig. 6. **(B)** qPCR data quantifying *CFTR* mRNA abundance in WT, G542X, and W1282X 16HBEs stably expressing PTBP1 and HNRNPL variants. The data is expressed relative to the scrambled control for each cell line = 1. Each column represents the mean ± SD of changes in expression; each symbol represents an individual data point normalized to *KRT18* or *PPIA* from at two independent experiments performed in quadruplicate (n = 16). Statistical analysis was performed using the Welch's unpaired *t*-test; **** indicates $p < 0.0001$ when comparing the control with the experimental cohort for each cell line.

protein isoform compared to the same cell lines expressing vector alone (Fig. 4B). We found that expression of each PTBP1 and HNRNPL variant led to 1.8- to 11.2-fold increases in *CFTR* mRNA abundance among the three cell lines compared to controls. Because expression of the RNA binding protein isoforms varied among the various cell lines, we were unable to quantitatively correlate the expression of specific isoforms with increases in *CFTR* mRNA abundance. However, qualitative examination of this data suggests that exogeneous expression of all PTBP1 and HNRNPL variants led to increases in *CFTR* mRNA abundance in all three cell lines. However, expression of HNRNPL variants generally had a greater impact on *CFTR* mRNA abundance in the G542X and W1282X cells compared to WT. This data supports our claim that PTBP1 and HNRNPL normally protect *CFTR* mRNAs from degradation by NMD.

4. Discussion

NMD is a conserved, eukaryotic cellular mRNA surveillance pathway. NMD not only degrades mRNAs harboring a PTC formed by a genomic mutation, but also targets physiological transcripts containing PTCs generated by alternatively spliced exons or upstream opening reading frames (uORFs), as well as transcripts with a long 3' UTR, for decay. NMD plays an important role in controlling gene expression, regulating ~10 % of the mammalian transcriptome [21].

PTC-containing transcripts are primarily degraded by the classical, exon junction complex (EJC) dependent branch of NMD that is mediated by a set of NMD factors bound to a PTC (UPF1 and the SMG complex) as well as additional NMD factors bound to EJCs (UPF2 and UPF3B), which are deposited onto transcripts 20–24 nucleotides upstream of each exon-exon junction during splicing [22].

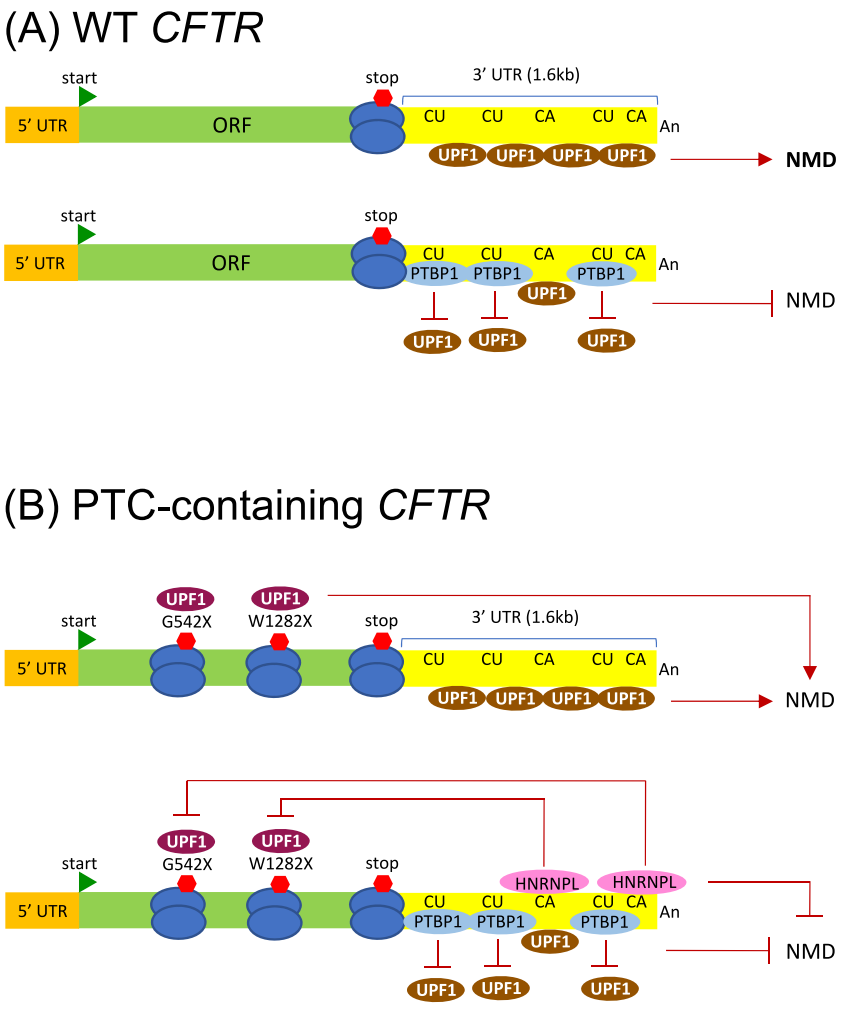

Fig. 5. Model of how PTBP1 and HNRNPL may regulate NMD of *CFTR* mRNAs. (A) PTBP1, but not HNRNPL, regulates WT *CFTR* mRNA abundance, likely by protecting these transcripts from EJC-independent NMD that is mediated by the accumulation of UPF1 on the long 3′ UTR. **(B)** Both PTBP1 and HNRNPL regulate PTC-containing *CFTR* mRNA abundance, suggesting that PTC-containing *CFTR* transcripts may be subject to both EJC- and long 3′ UTR-mediated NMD. We speculate that PTBP1 may protect *CFTR* mRNAs from 3′ UTR mediated NMD, while HNRNPL may protect *CFTR* mRNAs from EJC-mediated NMD that likely recruits different NMD-associated factors based on the location of the PTC. CU and CA represent binding motifs for PTBP1 and HNRNPL, respectively.

Normally, EJCs are removed from mRNAs by transiting ribosomes during the first round of translation, leading to remodeling and subsequent stabilization of the mRNA. However, if a PTC is present in an mRNA, translation will end at the PTC and any EJCs downstream of the PTC will remain bound to the mRNA. In this event, the interaction between PTC-bound NMD factors and downstream EJC-bound NMD factors leads to the recruitment of decay factors that degrade the mRNA.

The degradation of transcripts triggered by long 3′ UTRs is not as well characterized as EJC-mediated NMD. It has been shown that the NMD factor UPF1, an ATP-dependent RNA helicase, not only associates at PTCs, but also binds nonspecifically throughout the body of an mRNA [12]. Due to its displacement from the mRNA by ribosomes during translation, UPF1 rebinds and accumulates on 3′ UTRs. UPF1 becomes especially enriched on long 3′ UTRs, enabling decay factors to be recruited independently of EJCs. The Hogg group found that in HEK293 cells, the mRNA binding proteins PTBP1 and HNRNPL protect thousands of mRNAs from NMD by displacing UPF1 from the 3' UTR [5]. Because *CFTR* is not expressed in HEK293 cells, it could not have previously been identified by the Hogg study as a protected transcript.

PTBP1 and HNRNPL belong to the heterogenous nuclear ribonucleoprotein (HNRNP) family of mRNA binding proteins that shuttle between the nucleus and cytoplasm to regulate multiple stages of mRNA processing, transport, and metabolism *(15)*. These proteins are best known for their ability to associate with pre-RNAs in the nucleus to control alternative splicing of specific mRNA substrates. However, PTBP1 and HNRNPL also function in the cytoplasm, where they affect mRNA localization, stability, and translation of specific mRNA substrates *(15)*. To our knowledge, no role for PTBP1 or HNRNPL has previously been reported pertaining to the regulation of *CFTR* mRNA abundance or decay. One previous study did show PTBP1 may control alternative splicing of *CFTR* exon 9 as its overexpression led to increased exon skipping of exon 9 *in vitro (25)*. The G542X and W1282X mutations are in *CFTR* exons 11 and 23, respectively. We tested several *CFTR* qPCR primer sets and did not observe evidence of alternatively spliced forms of *CFTR* when we performed qPCR melt curves in 16HBEs with or without altered PTBP1 or HNRNPL expression (data not shown). However, we did not test for each possible splice site variant and thus, cannot rule out the possibility that *CFTR* splicing may be altered by PTBP1 and/or HNRNPL.

Our data suggest PTBP1 and HNRNPL protect human *CFTR* PTC-containing mRNAs from being degraded by NMD. We base this conclusion on the following results: 1) human *CFTR* mRNA possesses similar features as NMD substrates protected by PTBP1 and/or HNRNPL, including a long 3' UTR that contains potential PTBP1 and HNRNPL binding motifs; 2) depletion of PTBP1 or HNRNPL both reduced G542X and W1282X *CFTR* mRNA abundance, consistent with PTBP1 and HNRNPL protecting *CFTR* transcripts from NMD; 3) mRNA half-life studies show that loss of PTBP1 or HNRNPL increased the rate of *CFTR* G542X mRNA decay, suggesting that they influence *CFTR* mRNA abundance specifically *via* the rate of mRNA turnover; 4) exogenous expression of PTBP1 or HNRNPL significantly increased G542X and W1282X *CFTR* mRNA abundance, again supporting our hypothesis that these mRNA binding proteins protect *CFTR* mRNA from NMD. Together, this evidence strongly suggests that PTC-containing *CFTR* transcripts are protected from NMD by both PTBP1 and HNRNPL.

Notably, we also found that WT *CFTR* mRNA appears to be subject to NMD since its abundance increased with depletion of the core NMD factors UPF1, UPF2, or UPF3B. In addition, we found that depleting PTBP1, but not HNRNPL, reduced WT *CFTR* mRNA abundance and increased its decay rate. Moreover, exogenous expression of HNRNPL mediated a more robust impact on *CFTR* G542X or W1282X transcripts relative to WT. Together, these results suggest that PTBP1 and HNRNPL may protect different *CFTR* mRNAs based on how they are targeted to NMD (Fig. 5). PTC-containing transcripts could potentially undergo EJC or 3′ UTR mediated NMD (Fig. 5B), while WT *CFTR* would be expected to primarily by subject to 3′ UTR mediated NMD since it does not contain a PTC (Fig. 5A). PTBP1 affected both WT and PTC containing *CFTR* transcripts, suggesting that it may function in the 3′ UTR mediated NMD pathway. In contrast, HNRNPL mainly affected PTC-containing transcripts, suggesting that it may mediate how *CFTR* mRNAs are targeted to EJC-mediated NMD. It should also be noted that the presence of a uORF in the 5' UTR of the *CFTR* mRNA has also been shown affect its abundance *(26)*. Although this feature has not been shown to trigger NMD directly, we cannot rule out the possibility that it might influence the targeting of *CFTR* mRNAs to NMD and/or could influence how PTBP1 and HNRNPL regulate NMD of *CFTR* transcripts. Based on the ability of PTBP1 and HNRNPL to regulate mRNAs at multiple stages during their lifespan, we also cannot discount the possibility that PTBP1 and/or HNRNPL, in addition to protecting *CFTR* from turnover by NMD, may also regulate *CFTR* mRNA abundance through other mechanisms, such as transcription or mRNA localization.

Our data also suggest that *CFTR* transcripts are likely targeted to different branches of NMD depending on the position of the PTC. For example, we found that depletion of UPF1 and UP3B has a greater impact on G542X mRNA abundance, while UPF2 KD has a stronger effect on W1282X and WT *CFTR* mRNAs. This may also be related to the accumulation of UPF1 on regions downstream of the PTC, which is thought to create a faux 3' UTR that initiates NMD of transcripts lacking introns, such as most transcripts expressed in yeast [23]. Overall, our results suggest that different *CFTR* mRNAs are likely targeted for decay by several branches of NMD, which are mediated by different sets of factors. Notably, we attempted to better understand how PTBP1, HNRNPL, and UPF1 interact to modulate *CFTR* mRNA decay by simultaneously co-transfecting siRNAs into 16HBEs to perform double knockdowns (KDs) of PTBP1 and HNRNPL, PTBP1 and UPF1, or HNRNPL and UPF1; however, the double KDs led to cell inviability (data not shown). Future experiments are warranted to better understand how different PTBP1 and HNRNPL isoforms coordinate protection of various *CFTR* mRNAs from NMD.

NMD represents a potential therapeutic target for increasing the pool of PTC-containing mRNAs and subsequently, increasing the abundance of functional truncated proteins or enhancing the efficiency of therapies aimed at rescuing full-length, functional protein from PTC-containing mRNAs. However, implementing NMD inhibition as a therapeutic strategy has been hindered by a lack of NMD inhibitors with drug-like properties and concerns for whether global NMD can be inhibited for long periods without harmful side-effects. Apprehension toward the safety of NMD inhibition stems from studies showing: 1) knockout mutations of several core NMD factors is embryonically lethal in mice [24–26]; 2) attenuation of NMD during embryonic development prevents normal immune

system formation in mice [27]; and 3) neurodevelopmental disorders are associated with mutations in core NMD factors [28]. More recently, a mouse model in which NMD was attenuated after completion of embryonic development showed that after one month of NMD inhibition: 1) moderate NMD inhibition did not cause overt abnormalities; 2) strong NMD inhibition caused immunological abnormalities, and increased bone density in female mice; and 3) NMD substrates in neurological tissues are more sensitive to NMD perturbation than other somatic tissues [29]. Together, these findings suggest that globally inhibiting NMD is unlikely to be a feasible long-term therapeutic strategy. Rather, more targeted approaches to inhibit NMD for a subset of substrates, or for a specific substrate, will likely be required for safe implementation of NMD inhibition as a therapy. A better understanding of how mRNAs are targeted to NMD is needed to find safe and effective ways to inhibit their decay. The current study found that the mRNA binding proteins PTBP1 and HNRNPL help regulate the targeting of *CFTR* mRNAs to NMD. PTBP1 and HNRNPL may therefore represent therapeutic targets that can be manipulated to increase *CFTR* mRNA abundance. One can envision identifying/designing small molecules that allow PTBP1 and HNRNPL to protect *CFTR* mRNAs to a greater extent. Future experiments will be required to determine how PTBP1 and HNRNPL protect *CFTR* mRNAs from NMD.

FUNDING

Cystic Fibrosis Foundation KEELIN20G0 and KEELIN22G0.

Data availability statement

The data in this study has not been deposited to a publicly available repository because it will be made available upon request from the corresponding author.

CRediT authorship contribution statement

Amna Siddiqui: Validation, Methodology, Formal analysis, Data curation. **Arpit Saxena:** Validation, Methodology, Data curation. **Joshua Echols:** Visualization, Methodology, Data curation. **Viktoria Havasi:** Methodology, Data curation. **Lianwu Fu:** Writing – review & editing, Visualization, Validation, Methodology, Investigation, Data curation. **Kim M. Keeling:** Writing – review & editing, Writing – original draft, Visualization, Validation, Supervision, Project administration, Methodology, Investigation, Funding acquisition, Formal analysis, Data curation, Conceptualization.

Declaration of competing interest

The authors declare that they have no known competing financial interests or personal relationships that could have appeared to influence the work reported in this paper.

Acknowledgements

I wish to thank the UAB Gregory Fleming James Cystic Fibrosis Research Center for providing reagents and technical expertise. I also extend my thanks to the Bedwell Lab in the UAB Department of Biochemistry & Molecular Genetics for access to equipment, reagents, and helpful scientific discussions.

Appendix A. Supplementary data

Supplementary data to this article can be found online at https://doi.org/10.1016/j.heliyon.2023.e22281.

References

[1] O. Laselva, et al., Small-molecule drugs for cystic fibrosis: where are we now? Pulm. Pharmacol. Ther. 72 (2022), 102098.
[2] C. Ferec, G.R. Cutting, Assessing the disease-liability of mutations in CFTR, Cold Spring Harb Perspect Med 2 (12) (2012) a009480.
[3] Y.S. Oren, et al., The suppression of premature termination codons and the repair of splicing mutations in CFTR, Curr. Opin. Pharmacol. 34 (2017) 125–131.
[4] J.J. Porter, C.S. Heil, J.D. Lueck, Therapeutic Promise of Engineered Nonsense Suppressor tRNAs, vol. 12, Wiley Interdiscip Rev RNA, 2021, p. e1641.
[5] S.E. Fritz, et al., The RNA-binding protein PTBP1 promotes ATPase-dependent dissociation of the RNA helicase UPF1 to protect transcripts from nonsense-mediated mRNA decay, J. Biol. Chem. 295 (33) (2020) 11613–11625.
[6] Z. Ge, et al., Polypyrimidine tract binding protein 1 protects mRNAs from recognition by the nonsense-mediated mRNA decay pathway, Elife 5 (2016), e11155.
[7] A. Kishor, Z. Ge, J.R. Hogg, hnRNP L-dependent protection of normal mRNAs from NMD subverts quality control in B cell lymphoma, EMBO J. 38 (3) (2019), e99128.
[8] H.C. Valley, et al., Isogenic cell models of cystic fibrosis-causing variants in natively expressing pulmonary epithelial cells, J. Cyst. Fibros. 18 (4) (2019) 476–483.
[9] J. Kim, et al., AMPK and mTOR regulate autophagy through direct phosphorylation of Ulk1, Nat. Cell Biol. 13 (2) (2011) 132–141.
[10] M.M. Keenan, et al., Nonsense mediated RNA decay pathway inhibition restores expression and function of W1282X CFTR, Am. J. Respir. Cell Mol. Biol. 61 (2019) 290–300.

[11] K.J. Livak, T.D. Schmittgen, Analysis of relative gene expression data using real-time quantitative PCR and the 2(-Delta Delta C(T)) Method, Methods 25 (4) (2001) 402–408.
[12] J.R. Hogg, S.P. Goff, Upf1 senses 3'UTR length to potentiate mRNA decay, Cell 143 (3) (2010) 379–389.
[13] C. Mayr, Evolution and biological roles of alternative 3'UTRs, Trends Cell Biol. 26 (3) (2016) 227–237.
[14] E.J. Sanderlin, et al., CFTR mRNAs with nonsense codons are degraded by the SMG6-mediated endonucleolytic decay pathway, Nat. Commun. 13 (1) (2022) 2344.
[15] L.A. Clarke, et al., Integrity and stability of PTC bearing CFTR mRNA and relevance to future modulator therapies in cystic fibrosis, Genes 12 (11) (2021) 1810.
[16] C.Y. Cho, et al., PTBP1-mediated regulation of AXL mRNA stability plays a role in lung tumorigenesis, Sci. Rep. 9 (1) (2019), 16922.
[17] D.H. Lee, et al., hnRNP L binds to CA repeats in the 3'UTR of bcl-2 mRNA, Biochem. Biophys. Res. Commun. 382 (3) (2009) 583–587.
[18] C. Clerte, K.B. Hall, The domains of polypyrimidine tract binding protein have distinct RNA structural preferences, Biochemistry 48 (10) (2009) 2063–2074.
[19] S. Bhattacharya, et al., Structural basis of the interaction between SETD2 methyltransferase and hnRNP L paralogs for governing co-transcriptional splicing, Nat. Commun. 12 (1) (2021) 6452.
[20] L.M. Arake de Tacca, et al., PTBP1 mRNA isoforms and regulation of their translation, RNA 25 (10) (2019) 1324–1336.
[21] N.A. Sharifi, H.C. Dietz, Physiologic substrates and functions for mammalian NMD, in: L.E. Maquat (Ed.), Nonsense-Mediated mRNA Decay, Landes Bioscience, Georgetown, Texas, 2006, pp. 97–109.
[22] T. Kurosaki, M.W. Popp, L.E. Maquat, Quality and quantity control of gene expression by nonsense-mediated mRNA decay, Nat. Rev. Mol. Cell Biol. 20 (7) (2019) 406–420.
[23] N. Amrani, et al., A faux 3'-UTR promotes aberrant termination and triggers nonsense-mediated mRNA decay, Nature 432 (7013) (2004) 112–118.
[24] S.M. Medghalchi, et al., Rent1, a trans-effector of nonsense-mediated mRNA decay, is essential for mammalian embryonic viability, Hum. Mol. Genet. 10 (2) (2001) 99–105.
[25] J. Weischenfeldt, et al., NMD is essential for hematopoietic stem and progenitor cells and for eliminating by-products of programmed DNA rearrangements, Genes Dev. 22 (10) (2008) 1381–1396.
[26] D.R. McIlwain, et al., Smg1 is required for embryogenesis and regulates diverse genes via alternative splicing coupled to nonsense-mediated mRNA decay, Proc. Natl. Acad. Sci. U. S. A. 107 (27) (2010) 12186–12191.
[27] P.A. Frischmeyer-Guerrerio, et al., Perturbation of thymocyte development in nonsense-mediated decay (NMD)-deficient mice, Proc. Natl. Acad. Sci. U. S. A. 108 (26) (2011) 10638–10643.
[28] L.S. Nguyen, et al., Contribution of copy number variants involving nonsense-mediated mRNA decay pathway genes to neuro-developmental disorders, Hum. Mol. Genet. 22 (9) (2013) 1816–1825.
[29] J. Echols, et al., A regulated NMD mouse model supports NMD inhibition as a viable therapeutic option to treat genetic diseases, Dis Model Mech 13 (8) (2020) dmm044891. ETHICS DECLARATION Review and/or approval by an ethics committee was not needed for this study because no human subjects or animals were used in this study.